This is a repository copy of *Green and Chamomile Teas, but not Acarbose, Attenuate Glucose and Fructose Transport via Inhibition of GLUT2 and GLUT5*.

White Rose Research Online URL for this paper:
http://eprints.whiterose.ac.uk/120531/

Version: Accepted Version

Green and chamomile teas, but not acarbose, attenuate glucose and fructose transport via inhibition of GLUT2 and GLUT5

Jose A Villa-Rodriguez[1], Ebru Aydin[1,2], Julia S. Gauer, Alison Pyner, Gary Williamson[3], Asimina Kerimi.

School of Food Science and Nutrition, University of Leeds, Leeds, LS2 9JT, UK

Phone +44 113 3438380; Email: g.williamson@leeds.ac.uk

[1]Authors contributed equally to the work

[2]Current address: Süleyman Demirel University, Isparta, Turkey

[3]Corresponding author: g.williamson@leeds.ac.uk

Contribution of authors:

Planning and design of research for the paper: AK, GW, EA, JAVR

Experimental work: EA (transport experiments, enzyme inhibition); JAVR (transport experiments, enzyme inhibition, chamomile preparation, mRNA and protein expression); JG (expression in oocytes, oocyte transport); AP (sucrase inhibition using Caco-2 cells); AK (analysis of chamomile, transport experiments); GW, data analysis.

Writing of paper: All authors have contributed, read and agreed to the contents of the manuscript.

Abstract:

Scope: High glycaemic sugars result in blood glucose spikes, while high doses of post-prandial fructose inundate the liver, causing an imbalance in energy metabolism, both leading to increased risk of metabolic malfunction and type 2 diabetes. Acarbose, used for diabetes management, reduces post-prandial hyperglycaemia by delaying carbohydrate digestion.

Methods and results: Chamomile and green teas both inhibited digestive enzymes (α-amylase and maltase) related to intestinal sugar release, as already established for acarbose. However, acarbose had no effect on uptake of sugars using both differentiated human Caco-2 cell monolayers and Xenopus oocytes expressing human glucose transporter-2 (GLUT2) and GLUT5. Both teas effectively inhibited transport of fructose and glucose through GLUT2 inhibition, while chamomile tea also inhibited GLUT5. Long term incubation of Caco-2/TC7 cells with chamomile tea for 16 h or 4 days did not enhance the observed effects, indicating that inhibition is acute. Sucrase activity was directly inhibited by green tea and acarbose, but not chamomile.

Conclusion: These findings show that chamomile and green teas are potential tools to manage absorption and metabolism of sugars with efficacy against high sugar bolus stress, inflicted, for example, by high fructose syrups, where the drug acarbose would be ineffective.

Abbreviations:

ACN: acetonitrile

AMPK: 5' adenosine monophosphate-activated protein kinase

CPM: counts per minute

DMEM: Dulbecco's Modified Eagle's Medium

DMSO: dimethylsulfoxide

FBS: foetal bovine serum

GLUT: glucose transporter

GLUT2: glucose transporter SLC2A2

GLUT5: glucose transporter SLC2A5

PBS: sodium phosphate buffer

ROS: reactive oxygen species

TBP: tata-box binding protein

TBS: transport buffer solution

TEER: trans-epithelial electrical resistance

TFA: trifluoroacetic acid

INTRODUCTION

Fructose has received extensive interest as a potential risk factor for developing type 2 diabetes, but the long-term metabolic complications of fructose consumption in humans are controversial. Dietary fructose absorption is very efficient in the small intestine, mediated by the GLUT2 and GLUT5 transporters. Fructose transport by GLUT5 is a major factor for generation of fructose-induced hypertension, as demonstrated in glut5 -/- mice [1]. High levels of post-prandial fructose lead to rapid influx into the liver from the small intestine; as it bypasses hormonal signalling control, blood post-prandial fructose concentration does not rise in the same way as evidenced for glucose. This precipitates an inundation effect that can ultimately overload energy-related metabolic pathways. Fast processing of fructose by hepatic fructokinase C generates ample substrates for de novo lipogenesis leading to rising levels of uric acid and reactive oxygen species (ROS) [2], upregulated fructokinase expression [3] and inhibition of 5' adenosine monophosphate-activated protein kinase (AMPK) activity by elevated AMP [4]. However, epidemiological studies indicate that high fructose diets per se are not associated with an increased risk of hyperuricemia [5], implying that the stress from the rapid influx of fructose following repeated high bolus meals is a key factor in setting the liver functions at increased risk. According to numerous studies, high glycaemic index diets, even with equivalent total carbohydrate, lead to increased risk of diabetes and cardiovascular risk [6, 7]. High post-prandial glucose long-term gives rise to endothelial dysfunction, increased ROS production by complex I, and a plethora of changes in cell signalling and gene expression [8, 9]. Dietary fructose is mostly consumed with glucose, either in the form of sucrose or as high fructose corn syrups. Sucrose consists of glucose linked to fructose, and in the intestine, the brush border enzyme sucrase-isomaltase hydrolyses sucrose into its constituent sugars [10], which are then absorbed by GLUT transporters as the free sugars. Acarbose is a drug routinely used to manage carbohydrate

digestion in diabetics, and acts by inhibiting the starch digesting enzymes α-amylase and enterocyte brush border α-glucosidases and sucrase [11]. Up to now it has not been clear if acarbose can also directly act on intestinal sugar absorption or sugar transporters.

Foods, herbal medicines and plant extracts, often overlooked in the clinical setting, can delay the need to resort to prescribed drugs by contributing to everyday health maintenance [12, 13] or even more by eliciting complementary effects to prescribed drugs. Management and blunting of fructose absorption, without modifying the total amount of absorbed dietary fructose, could provide a route to preventing fructose-induced liver inundation post-prandially and hence help to prevent some of the acute effects of fructose overload on liver metabolic processes [14]. Limiting the supply of fructose-derived lipogenic intermediates to the liver could restrict necessary substrates for excess AMP and uric acid production to below threshold and hence delay the onset of associated disease manifestations. If the same foods or beverages were able to attenuate starch digestion and glucose absorption, the potential beneficial effect would be significantly magnified. Certain polyphenols have been suggested to modify carbohydrate digestion and sugar absorption [15]. Chamomile (Matricaria recutita, also "German chamomile"), traditionally used for its "digestive" properties, has been reported to inhibit sucrase activity and decrease plasma glucose chronically in streptozotocin-induced diabetic rats [16], to interact with PPARs and improve fatty liver in high fat-fed C57BL/6 mice [17], and to decrease glycosylated haemoglobin, serum insulin, homeostatic model assessment for insulin resistance, and serum malondialdehyde in type 2 diabetic patients [18]. Green tea (Camellia sinensis) can also improve glucose tolerance in healthy young men [19] and in rats fed a high-fat diet [20] while some of the constituent catechins can inhibit α-amylase [21]. We therefore directly compared the effects of chamomile and green tea to acarbose and further examined their mechanism of action on fructose and glucose intestinal absorption, using a combination of models: the well characterised differentiated

Caco-2 and Caco-2/TC7 cell monolayers, enzyme inhibition assays and oocyte-expressed sugar transporters. The Caco-2 and Caco-2/TC7 cell models have been extensively characterised, and have been utilised for studies on sugar transport as a model for the small intestine, since the expression and membrane location of GLUTs and SGLT1 is well known under a wide variety of conditions [22, 23]. In addition, the pathways for utilisation of fructose are intact since fructose can be readily used as an energy source by Caco-2 cells [24]. Here we demonstrate that chamomile and green teas have additional and complementary activities on sugar transport not exhibited by acarbose.

MATERIALS AND METHODS

Radiolabelled sugars

2-[^{14}C(U)]-deoxy-D-glucose, D-[^{14}C(U)]-glucose and [^{14}C(U)]-sucrose were from Perkin Elmer (Boston, USA), D-[^{14}C(U)]-fructose was from Hartmann Analytic (Braunschweig, Germany), D-glucose and D-fructose were from Fisher Scientific Ltd (Leicestershire, UK), and sucrose was from Sigma (Dorset, UK).

Analysis of the chamomile and green teas

Chamomile and green tea were supplied as standard dried extracts by PhytoLab & Co (Vestenbergsgreuth, Germany). Matricaria recutita ("German" chamomile) was extracted with 60% ethanol and dried, and contained added maltodextrin (50% by weight) to enhance dispersion and solubilisation. Camellia sinensis (green tea) was an aqueous extract from leaves, and dried with no additional components. Each extract was dissolved in transport buffer solution (TBS; 5.4 mM potassium chloride, 0.441 mM potassium phosphate, 0.352 mM sodium phosphate dibasic, 4.2 mM sodium bicarbonate, 1.8 mM calcium chloride dehydrate, 0.1 mM ascorbic acid and 137 mM sodium chloride, pH adjusted to 7.4 with 1M

HCl before sterile filtration) to make 10 mg/ml and centrifuged at 17,000 g for 5 min. The final extract concentration was corrected for the maltodextrin content. In preliminary experiments, we demonstrated that the relevant concentrations of maltodextrin did not interfere in any of the transport assays, but affected the digestive enzyme assays, and it was therefore removed chromatographically as described below, before testing in α-amylase and α-glucosidase assays.

Compositional analysis of green tea

Analysis of the green tea was performed by reversed phase high performance liquid chromatography (HPLC) on an Agilent 1200 series system (Agilent Technologies, Dorset, UK). Samples (5 µl) were injected on an Eclipse plus C18 column (30 °C, 2.1 mm x 100 mm, 1.8 µm; Agilent Technologies) and separation was achieved on a gradient of 0.1% formic acid in MilliQ water (Solvent A) and 0.1% formic acid in acetonitrile (Solvent B). Elution started at 10% B at a flow rate of 0.25 ml/min and increased to 15% after 9.5 min, and after 14.5 min to 95%. Standard curves were run with commercially available standards for all compounds and used to determine concentrations, with taxifolin as the internal standard (10 µg/ml).

Compositional analysis of chamomile

Analysis of chamomile was carried out by liquid chromatography-mass spectrometry on a Vanquish UHPLC-TSQ Quantiva triple quadrupole system (Thermo Scientific, Santa Clara, USA) with an Accucore Vanquish C18+ column (2.1 mm x 100 mm, 1.5 µm; Thermo Scientific) at a flow rate of 0.3 ml/min. Solvent A was MilliQ water containing 0.1% formic acid and solvent B was acetonitrile containing 0.1% formic acid. All solvents were of mass spectrometry grade (VWR, Leicestershire, UK). Compounds were eluted with the following

gradient: 0 min: 5% B, 0-5.5 min linear from to 50% B, 5.5-6 min linear from to 95% B, 6-7 min isocratic at 95% B, 7-7.1 min linear to 5% B and 7.1-9 min isocratic at 5% B. Fragmentor voltages and collision energies were optimised for each compound using pure standards obtained from PhytoLab & Co (Vestenbergsgreuth, Germany).

Preparation of maltodextrin-free chamomile.

For enzyme inhibition studies, the maltodextrin in the chamomile preparation was removed using an ÄKTA Purifier System (GE Healthcare, Fairfield, CT, USA) controlled by a PC running GE Unicorn software (5.11) equipped with a µRPC C2/C18 ST semi-preparative column (4.6x100 mm I.D., 5 µm; GE Healthcare, Fairfield, CT, USA). Chamomile prepared in MilliQ water was loaded manually using a syringe through a sample loop of 0.1 ml and eluted using MilliQ water containing 0.1% TFA (solvent A) and ACN (Solvent B) at a flow rate of 0.75 ml/min as follows: 0-3 min linear gradient from 5 to 24% B; 3-6 min isocratic at 24% B; 6-18 min linear gradient to 40% B; 18-24 min isocratic at 40%B, 24-30 min linear gradient to 100% B: 30-35 min isocratic at 100% B, 35-38 min linear gradient to 5% B, 38-41 min isocratic at 5% B . The elution was followed at 280 nm and the polyphenol maltodextrin-free fraction was collected. Combined fractions from multiple runs were freeze-dried and stored at -20 °C.

Cell culture

The Caco-2 cell line (HTB-37) was obtained from the American Type Culture Collection (LGC Promochem, Middlesex, UK). Cells were routinely cultured in normal glucose Dulbecco's Modified Eagle's Medium (5.5 mM, DMEM) supplemented with 15% (v/v) Fetal Bovine Serum (FBS), 100 U/ml penicillin, 0.1 mg/ml streptomycin, and 0.25 µg/ml

amphotericin B at 37°C with 10% CO_2 in a humidified atmosphere. All cell culture reagents were from Sigma (Sigma Aldrich, Gillingham, UK) unless otherwise stated.

Radiolabelled sugar transport experiments

For transport experiments, cells were seeded on 6-well Transwell plates (Corning 3412, Appleton Woods, Birmingham, UK) at a density of 6.43 x 10^4 cells/cm^2 until full differentiation of the monolayer (21 - 23 days). A minimum of four to six replicate wells were allocated per treatment per experiment. Cells were washed with TBS and growth medium was replaced with 2 ml of TBS in both apical and basolateral compartments and cells were incubated for 30 min (37 °C, 10% CO_2). Monolayer integrity was assessed by measurement of the trans-epithelial electrical resistance (TEER) with a Millicell ERS voltohmmeter (Merck Millipore UK). Wells with a resistance exceeding a blank membrane by 300 Ω were used for experiments. Fresh TBS solution containing the test sugar and 0.045 µCi/ml ^{14}C-labelled sugar with or without the test substance (pH adjusted to 7.4) was added to the apical or basolateral compartment and cell monolayers were further incubated; 25 min for glucose, 60 min for fructose and sucrose transport experiments. TEER values were measured again and solutions from apical and basolateral compartments were mixed with 5 ml of scintillation liquid (Gold Star, Meridian Biotechnologies, Surrey, UK) for radioactivity measurements with a Packard 1900 TR Liquid Scintillation Analyser. A calibration curve of radioactivity as a function of known amounts of [^{14}-C]-sugar was prepared from the same test solution(s). Cell suspensions were also collected in 1 M NaOH and neutralised before radioactivity measurements. To assess the long-term effect of chamomile on sugar transport, cells were pre-incubated for 12 h or 96 h and the assay was repeated as described above (between 21-23 days).

Inhibition of sugar transport using differentiated Caco-2/TC7monolayers

To further study the inhibition of GLUT2 transport by chamomile extract, the Caco-2/TC7 clone was used. Caco-2/TC7 cells were a kind gift from Prof. Monique Rousset, (INSERM, France). Cells were grown and maintained in the same medium as described above with 25 mM glucose which favours higher apical baseline levels of GLUT2 [25, 26]. For experiments, cells were seeded at a density of 6.25×10^4 cells/cm^2 in 12-well Transwell plates (Corning 3401, Appleton Woods) and cultured for 21-23 days as above. After 7 days, cells on the apical side were maintained in the same medium without FBS for the rest of the differentiation period. Glucose transport experiments were carried out as described above and 0.5 ml of TBS containing glucose and 0.15 µCi/ml with and without chamomile extract was added to the apical side and 1 ml TBS in the basal compartment. The glucose transport experiments were repeated where stated under Na$^+$-free conditions to delineate the involvement of SGLT1.

Estimation of α-amylase and α-glucosidase activities

For inhibition assays, maltodextrin-free stock solutions of chamomile were reconstituted in DMSO. The maximum DMSO concentration (5%) in the assay did not affect the enzyme activity as assessed in control incubations. Inhibition of human salivary α-amylase was tested as previously described [27]. Maltase, sucrase and isomaltase assays were conducted as before [28] with some modifications. An acetone extract from rat small intestine was used as the enzyme source and the assays were optimised for linearity in terms of enzyme and substrate concentration. The reaction mixture contained 200 µL of enzyme solution (4 mg/ml in 0.01 M phosphate buffer, pH 7 for maltase and 20 mg/mL for sucrase and isomaltase), 200 µl of substrate (final 3 mM maltose, 16 mM sucrose and 6 mM isomaltose), 50 µl of test inhibitor (various concentrations) and 50 µl of 0.01 M, pH 7, phosphate buffer (PBS). The enzyme

solution and the assay mixture containing the maltose, inhibitor and PBS were pre-incubated (37 °C, 10 min) and the reaction started by addition of the enzyme. The reaction (20 min) was stopped by placing the assay mixture in a boiling water bath (100 °C, 10 min) before cooling to room temperature and removing the test inhibitors by solid phase extraction (Oasis MAX, Waters, Elstree, UK) as described for α-amylase [27]. The glucose produced was determined by the hexokinase assay. Briefly, 10 µL of the reaction mixture were transferred to a 96 well plate (Greiner UV-star M3812, Sigma) followed by the addition of 250 µL of hexokinase reagent. Following incubation (15 min, 30 °C) the absorbance was recorded at 340 nm on a PHERAstar FS microplate reader (BMG LABTECH, Germany). For assays of human sucrase, Caco-2/TC7 cell lysates were used as the enzyme source. Caco-2/TC7 cells were routinely cultured as described above in DMEM medium without glucose (Gibco 11966, Life Technologies Thermo Fisher Scientific, Paisley, UK), supplemented with 25 mM sucrose and 20% (v/v) FBS. 75 cm^2 culture flasks were seeded, and cells allowed to differentiate for 21 days with medium replaced every other day. Cells were washed three times with cold PBS and scraped in 1 ml of PBS containing protease inhibitors (P8340, Sigma, UK). Cell lysates stored at -80 °C were thawed on the day of the assay, vortexed and passed 10-15 times though a 21G needle syringe. The protein content was determined by the Bradford Assay in a well plate format (23200, Thermo Fisher Scientific, UK). The assay was optimised for incubation time (10 min), linearity in terms of enzyme (160 µg of total protein) and substrate concentration (10 mM sucrose), and was performed as described above. Rates were calculated relative to controls with no substrate and no enzyme.

Expression of GLUT5 in oocytes

The GLUT5 gene-containing region was extracted from SLC2A5 in pANT7_cGST plasmid (DNASU Plasmid Repository, Arizona State University, USA) employing PCR reactions

with specific primers. The product was inserted into a linear pBF plasmid, an amphibian expression vector, using In-Fusion cloning kits (638909 Clontech, Temple, AZ, USA). Linearization of the pBF plasmid was carried out with XbaI (RG181 Promega, Madison, WI, USA). Specific forward and reverse primers with homologous ends to GLUT5 containing sequence as well as ends of linear pBF plasmid were 5'-GGT TAA CTA GTC CGA ACC ACG GGG ACG TG- 3' and 5' -CGA TGA ATT CTA TCA CAA CTG TTC CGA AG- 3' (Sigma, UK). The resulting plasmids were transformed into Stellar™ Competent Cells (E. coli HST08 strain) and incubated on agar plates (37 °C, 16-18 h) containing ampicillin. Plasmids containing GLUT5 were linearized with MluI (RG381 Promega, Madison, WI, USA) and transcribed in vitro using SP6 polymerase mMESSAGE mMACHINE® (AM1340 Ambion, Applied Biosystems, Warrington, UK). Final mRNA concentration was determined with a Nanodrop ND100 spectrophotometer (Labtech, Thermo Fisher) and 1 µl of RNA product was run on 1.5%, 2.2 M formaldehyde gel to verify the size of the product. X. laevis oocytes were isolated and microinjected as previously described [29]. Ovary from adult females was purchased from the European Xenopus Resource Centre (University of Portsmouth, UK) and a quarter of the ovary was incubated in 5 ml calcium-containing OR2 solution with 1 mg/ml collagenase A (10103578001 Roche, Burgess Hill, UK) at room temperature for 90 min or until fully digested. The digest was washed and kept in OR2 plus antibiotics medium at 18 °C until microinjection. Stage V oocytes were microinjected with 50 nl of mRNA or water, to serve as controls, using an air pressure injector and incubated in OR2 medium with antibiotics at 18 °C for 24 h before experiments. Sugar uptake experiments were executed with 6 replicates of three oocytes in 6 mM-fructose containing 0.5 µCi D-[^{14}C(U)] fructose, at 37 °C for 15 min, or in 100 µM fructose solution containing 0.5 µCi at 25 °C for 5 min. To stop the reaction, oocytes were washed with ice cold fructose of the same concentration as in the incubation step. Three oocytes per replicate were then

homogenised together in 0.3 M sucrose containing 10 mM sodium phosphate (pH 7.4) and

protease inhibitors. Nuclei and debris were pelleted from homogenized samples by

centrifugation at 3,000 x g (15 min, 4 °C). The supernatant was centrifuged at 48,000 x g (1 h

at 4 °C) to pellet the membranes, which were re-suspended in 0.3 M sucrose containing 10

mM sodium phosphate and protease inhibitors. The supernatant from the second

centrifugation step was transferred to a scintillation vial and mixed with 5 ml of scintillation

liquid (Gold Star, Meridian Biotechnologies). Radioactivity was measured on a Packard Tri-

Carb 1900 TR Liquid Scintillation Counter. Glut5 protein expression was confirmed in the

oocyte membrane fraction with ProteinSimple WES (ProteinSimple, Bio-Techne, UK)

according to manufacturer's instructions. Samples were denatured at 37 °C for 15 min and

primary antibody incubation time was 30 min. The GLUT5 antibody (sc271055 Santa Cruz

Biotechnology, Dallas, TX, USA) was used at a dilution of 1:50 and the secondary antibody

(mouse, ProteinSimple) was used neat as supplied. Optimal loading concentration for GLUT5

microinjected oocyte membrane samples was 0.2 mg protein/ml.

Expression of GLUT2 in oocytes

Expression of GLUT2 in oocytes followed a similar protocol to that described above for

GLUT5. GLUT2 gene containing region was extracted from pcDNA3.2/v5-DEST hGlut2

plasmid (Addgene, Cambridge, MA, USA) and inserted into linear pBF. Specific forward and

reverse primers sequences used were 5' -CCG GGT TAA CTA GTC CCA CTG CTT ACT

GGC TTA TC- 3' and 5' -TAT CGA TGA ATT CTA TCA GGG TTC CTT CCG GTA TTG

TC- 3', respectively. GLUT2 containing plasmids were linearized with PmlI (R05325 New

England Biolabs, Hitchin, UK) and in vitro transcribed. Following microinjection, oocytes

were incubated in OR2 medium with antibiotics at 18 ˚C for 48 h before experiments were

performed. All sugar uptake experiments were conducted with 6 replicates of three oocytes in

100 µM glucose solution containing 0.5 µCi of D-[^{14}C(U)]-glucose at 25 °C for 5 min. Protein detection was confirmed with ProteinSimple WES using a GLUT2 antibody (ab95256 Abcam Cambridge, UK) at 1:50 dilution. The optimal loading concentration of GLUT2 microinjected oocyte membrane samples was 0.4 mg/ml.

Quantitation of GLUT5 mRNA and protein in CaCo-2 and CaCo-2/TC7 cells

For GLUT5 mRNA and protein expression analysis, CaCo-2 and CaCo-2/TC7 cells were seeded on solid supports at a density of 6.43 x 10^4 cells/cm^2 and maintained for 23 d before harvesting. RNA isolation was performed using the RNAqueous-4PCR kit (AM1912, Ambion, Life Technologies, Thermo Fisher Scientific, Paisley, UK) and RNA concentration and quality was determined with a Nanodrop 1000ND spectrophotometer (Labtech, Thermo Fisher Scientific). 1 µg of RNA was reverse transcribed to cDNA using a High Capacity RNA-to cDNA master mix kit (Life Technologies).

Quantitative gene expression was carried out by droplet digital PCR on a QX100 system (Bio-Rad, Watford, UK). Briefly, 20 µL of sample containing 8 µL of diluted cDNA (21.5 ng) with RNAse, DNAse free Milli-Q water, 1 µL of GLUT5 FAM-labelled TaqMan primer (Hs01086390_m1, Life Technologies), 1 µL of VIC-labelled TaqMan primer of TBP (TATA-Box Binding Protein, Hs00427620_m1, Life Technologies) and 10 µL of droplet digital PCR Supermix for Probes (no dUTP, Bio-Rad) were introduced in the sample well for droplet generation. TBP was used as a reference for the same group of samples to compare performance between ddPCR runs. Droplets were generated according to the manufacturer's procedure with the QX100 Droplet generator (Bio-Rad) and transferred to a C1000 PCR (Bio-Rad). The average number of accepted droplets was 14781 ± 981. The data was analyzed with the QuantaSoft software (Kosice, Slovakia).

For analysis of GLUT5 protein, the ProteinSimple WES system was used as described above, but the incubation time for the primary antibody was 1 h and for the secondary 30 min. Different concentrations of cell lysates were tested to determine linearity of GLUT5 and Claudin-1 (mouse, monoclonal, 2H10D10, Invitrogen, Thermo Fisher Scientific), and both antibodies were used at a dilution of 1:50 for detection in the same capillary. A separate standard curve was constructed for each cell line. Optimal loading concentration of cell samples was determined as 0.1 and 0.05 mg/ml for CaCo-2 and CaCo-2/TC7 cells respectively. Quantification of peak areas and gel-like image reconstruction was carried out using the ProteinSimple Compass software.

Data analysis

IBM SPSS Statistics v.24 was used for analysis of the data either by one-way ANOVA or independent samples t-test with additional details where necessary as noted in legends. Values shown represent the average between independent experiments and error bars indicate standard deviation (SD) unless otherwise stated.

RESULTS

Establishing optimum conditions for estimating fructose, glucose and sucrose transport across differentiated Caco-2 cell monolayers.

D-[^{14}C(U)]-fructose transport from the apical to basolateral compartment (Figure 1A) and cellular uptake (Figure 1B) was assessed using differentiated Caco-2 cell monolayers. D-[^{14}C(U)]-glucose transport (Figure 1C) and cellular uptake (Figure 1D) were also studied in the apical to basolateral direction. The rate of D-[^{14}C(U)]-glucose transport (linear with time for $\geq$ 60 min) was 1.8 nmol/min per well (surface area = 1.12 cm^3), and the dependence on glucose concentration followed clear Michaelis Menten kinetics with apparent K_m = 8.1 mM glucose and V_{max} = 0.09 µmol substrate transported/min. Cellular uptake of D-[^{14}C(U)]-glucose was characterised by a rapid uptake over the first 2 min. Sucrose is hydrolysed by brush border sucrase and the resulting products, fructose and glucose, are transported across the enterocytes. After incubation with [^{14}C(U)]-sucrose, the ^{14}C-label was transported apically to basolaterally (Figure 1E). The apical to basolateral transport was about 2-fold higher than in the reverse direction (Figure 1F).

Effect of acarbose on sugar transport across differentiated Caco-2 monolayers

Acarbose did not inhibit either glucose or fructose transport across differentiated Caco-2 cell monolayers using the optimised conditions described above. However, acarbose inhibited cellular sucrose transport efficiently in our model with an IC$_{50}$ value of ~7 µM (Table 1), owing to its ability to inhibit the brush border enzyme sucrase as previously reported (see below).

Effect of chamomile and green teas on sugar transport and uptake by differentiated Caco-2 cell monolayers

16

Several food and beverage extracts were screened (data not shown), and the two most active on inhibition of sugar transport, chamomile tea (German chamomile, Matricaria recutita) and green tea (Camellia sinensis) were selected. Chamomile inhibited the transport of D-[^{14}C(U)]-fructose from the apical to basolateral compartment (Figure 2A), and the dose-dependence of the effect (Figure 2B) allowed estimation of the IC$_{50}$ value for transport, which is shown in Table 1. Chamomile also dose-dependently inhibited the apical to basolateral transport of D-[^{14}C(U)]-glucose (Figure 2C) with a significant (p≤0.01) decrease in the cellular uptake of D-[^{14}C(U)]-glucose by ~30 % (Table 1). [^{14}C(U)]-sucrose transport was dose-dependently inhibited by chamomile (Figure 2D), both in differentiated Caco-2 cell monolayers and also in Caco-2/TC7 cells (Table 1), which express higher levels of sucrase activity [22]. During the transport experiments, tight junction integrity, assessed by TEER, was not modified by chamomile. Green tea extract also inhibited fructose, glucose and sucrose transport, the latter in both Caco-2 and Caco-2/TC7 cells (Table 1). Green tea also increased the tight junction integrity as shown by a ~20%.increase in TEER values.

Analysis of the main components of chamomile and green tea

We analysed the extracts to determine the profile of compounds present. Analysis of green tea by HPLC-UV DAD revealed that it contained (-)-epigallocatechin gallate (240 mg/g extract), (-)-epigallocatechin (70 mg/g extract), (-)-epicatechin (40 mg/g extract) and (+)-catechin (17 mg/g extract), consistent with published data. Analysis of the chamomile extract was considered essential given the different profiles of bioactives reported for chamomile before. LC-MS analysis was carried out based on specific MRM transitions as guided by a compilation of published literature on chamomile composition. A chromatogram showing traces of major identified components is shown in Figure 3 and their concentration based on standard curves with commercially available standards is shown in Table 2. Apigenin-7-O-

glucoside (12.3% dry weight) was found to be the most abundant compound followed by apigenin (0.28%). The compound(s) tentatively termed as phenolic glucoside(s) have not yet been conclusively identified in the literature.

Mechanism of action of chamomile on inhibition of glucose transport

Both chamomile and green tea decreased the transport (Figure 4A) and uptake (Figure 4B) of 2-[^{14}C(U)]-deoxy-D-glucose, a non-metabolisable derivative of glucose, indicating that a major part of the effect is on glucose transport directly rather than effects on metabolism. Caco-2 and Caco-2/TC7 cells express the sugar transporters GLUT2 (for glucose and fructose), GLUT5 (for fructose) and the sodium-dependent transporter SGLT1 (for glucose). In order to first examine the relative inhibition of SGLT1 compared to GLUT2, experiments were conducted on glucose transport using Na$^+$-free conditions. Both phloridzin and phloretin inhibited D-[^{14}C(U)]-glucose transport in differentiated Caco-2/TC7 cell monolayers in the presence of Na$^+$ (Figure 5A). Phloridzin is a well-established SGLT1 inhibitor, while phloretin inhibits GLUT2 [29-31] (Figure 5B). In the absence of Na$^+$, glucose transport was decreased by 35% (Figure 5C), implying that SGLT1 in Caco-2/TC7 cells is responsible for ~ 35 % of the total D-[^{14}C(U)]-glucose transported. This is corroborated by two observations; phloridzin showed no inhibition of D-[^{14}C(U)]-glucose transport under Na$^+$-free conditions (Figure 5C) and D-[^{14}C(U)]-glucose transport was dose-dependently affected by phloretin (IC$_{50}$ = 63±8 µM) (Figure 5A). Both findings also attest to the role of GLUT2 as the main glucose transporter in Caco-2/TC7 cells. Chamomile dose-dependently inhibited D-[^{14}C(U)]-glucose transport both in the presence and absence of Na$^+$ (Figure 5D). Under Na$^+$-free conditions, a reduction of ~ 50 % of the IC$_{50}$ value and an increase of ~ 20% of the maximum inhibition were observed (Figure 5D). These data suggest that SGLT1 is a minor component

in inhibition of glucose transport by chamomile, with most of the inhibitory effect linked to GLUT2.

Mechanism of action of chamomile on inhibition of fructose transport

Fructose transport is sodium independent as it is through GLUT2 and GLUT5, but not through SGLT1. Inhibition of $[^{14}C(U)]$-fructose transport by chamomile was ~50 % lower in Caco-2/TC7 cell monolayers compared to Caco-2 cells. To dissect the mechanism further, we quantified and compared the expression of GLUT5 in the two clones. GLUT5 protein was measured by automated capillary Western blotting. A standard curve was constructed for differentiated Caco-2 (Figure 6A) and Caco-2/TC7 (Figure 6B) cell samples relating the amount of total cellular protein against the specific peak area of the chemiluminescent signal based on antibody mass detection. A linear response was evident for both GLUT5 protein and the multiplexed internal control, Claudin-1, with amount of protein applied. Comparison of the amount of GLUT5 and Claudin-1 in each cell line is shown as an electropherogram view (Figure 6C) and as a reconstructed lane view (Figure 6D). Results obtained showed that GLUT5 protein was ~2.0-fold higher ($p \leq 0.01$) in the Caco-2/TC7 line (Figure 6E). Consistently, GLUT5 mRNA expression (Figure 6F) was also higher (~ 2.5-fold; $p \leq 0.01$). This characterization is consistent with the transport experiments, showing that chamomile is more effective at inhibiting fructose transport by interacting with GLUT2 compared to GLUT5.

Inhibition of GLUT5 and GLUT2 expressed in Xenopus oocytes

To establish further the mechanism of action, we expressed GLUT2 and GLUT5 in Xenopus oocytes and examined the inhibition by chamomile, green tea and acarbose. For GLUT5, L-sorbose-Bn-OZO used as a positive control at 6 mM [32] strongly inhibited D-$[^{14}C(U)]$-

fructose uptake into oocytes (Figure 7A). Acarbose did not inhibit D-[^{14}C(U)]-fructose uptake by GLUT5 in Xenopus oocytes up to the maximum concentration tested, at either high or low fructose concentrations (Figure 7B). Green tea did not inhibit uptake of fructose by GLUT5 (Figure 7C), whereas chamomile inhibited D-[^{14}C(U)]-fructose uptake by GLUT5 at the lower concentration of D-[^{14}C(U)]-fructose (Figure 7D and E). On the other hand, uptake of D-[^{14}C(U)]-glucose by Xenopus oocytes expressing GLUT2 was strongly inhibited by both chamomile (Figure 7F) and green tea (Figure 7C), but strikingly no inhibition was observed for acarbose (Figure 7C) even at the highest concentrations tested. Data are summarized in Table 3.

Effect of pre-incubation with chamomile on glucose, fructose and sucrose transport

To investigate if chamomile could exert an additional chronic effect on sugar transport on top of the acute effects observed, we tested a longer term incubation under several conditions (Figure 8). Incubation with chamomile for 16 h did not affect the transport or uptake of glucose or fructose, but led to a small but significant decrease in sucrose transport ($p \leq 0.05$) compared to the control (Figure 8A and B). Longer term incubation with chamomile for 96 h did not affect glucose transport (Figure 8C).

Inhibition of digestive enzymes

Acarbose was a potent inhibitor of brush border sucrase and of starch-digesting enzyme activities as expected; although it was found to be a much weaker inhibitor of brush border isomaltase activity. Chamomile and green tea extracts inhibited human salivary α-amylase and rat maltase activities, but only green tea inhibited rat isomaltase, rat sucrase and human sucrase activities (Table 3).

20

DISCUSSION

A chronic excess of dietary fructose leads to an increased risk of metabolic dysfunction. This is partly due to post-prandial pulses of fructose in the liver which cause immediate and substantial changes in ATP levels, giving rise to other metabolic changes including increased uric acid and ROS production [2, 33]. The drug acarbose is prescribed for diabetics, and is well established to act on carbohydrate digestion by inhibiting α-amylase and α-glucosidase activities [34]. In rats, acarbose did not modify expression of SGLT1 nor GLUT2, the major glucose transporters in the small intestine, but modulated GLUT1 expression. However, these changes did not modify overall glucose transport [35], and furthermore, acarbose did not inhibit monosaccharide transport in rats [36]. We show here that acarbose does not directly interact with human glucose and fructose transporters, GLUT2 and GLUT5, and does not inhibit glucose or fructose transport in differentiated Caco-2 cell monolayers. Acarbose would therefore be ineffective against fructose and glucose absorption from, for example, high fructose corn syrups, which contain ~50% glucose and ~50% fructose. On the other hand, acarbose would be effective in attenuating sucrose digestion as it inhibits sucrase activity as expected [36] and indirectly slows the rate of transport of the products across the brush border through diminished substrate concentration. Chamomile and green teas, owing to their ability to inhibit both glucose and fructose transport, could be particularly beneficial for reducing liver inundation by fructose at the gastrointestinal level in addition to blunting blood glucose spikes. We propose that this can present a new and effective means to manage fructose absorption, which is increased in diabetes, partly due to increased expression of gastrointestinal GLUTs. Evidence presented here shows that the effect of chamomile is acute, since no changes in glucose or fructose transport were observed after longer term treatment with chamomile. This means that an effect on glycaemia would only be possible when the chamomile or green tea were consumed at the same time as the carbohydrate. A very small

but statistically significant reduction was observed for sucrose transport following chronic incubation with chamomile. Since the enzyme sucrase catalyses the conversion of sucrose into glucose and fructose before transport, then it is possible that chamomile treatment produces a small reduction in expression of sucrase, even though chamomile was not an acute direct inhibitor of the enzyme.

The concentrations reported here as necessary for inhibition are comparable to that obtained from drinking a cup of brewed chamomile tea. If 3 g of flowers are typically added to ~100 ml boiling water, then the concentration of extracted matter in the drink would be about 3 mg/ml assuming 10% extraction. This is several-fold higher than the necessary concentration for 50% inhibition. Clearly in the case of supplements, the concentrations can be substantially higher depending on the type of supplement consumed and the dose. For green tea, the number of available products and brewing methods are vast, but if 2 g of tea is added to 100 ml water, then the concentrations required for inhibition would be readily obtained by drinking tea, and again, much higher concentrations could be achieved by taking supplements.

The proposed mechanism of inhibition is summarised in Figure 9 for chamomile and for acarbose. Acarbose strongly inhibits α-amylase and α-glucosidase enzymes while no effect was evident on glucose or fructose transport, presumably because the tetrasaccharide structure of acarbose is too large to fit into the active site of monosaccharide transporters. Chamomile attenuates fructose transport across Caco-2 cells in a dose-dependent manner primarily through GLUT2 inhibition, but with some effect on GLUT5. The mild inhibition of GLUT5 accounts for the lack of total inhibition of fructose transport across the Caco-2 cells by chamomile, which does not reach 100%. The other main sugar transporter, SGLT1, does

not transport fructose [37]. For glucose transport, we propose that inhibition of transport by chamomile is mostly a result of GLUT2inhibition based on data from GLUT2 expression in Xenopus oocytes, and in Caco-2/TC7 cells where the GLUT2 transport component was strongly inhibited by both phloretin (a known GLUT2-specific inhibitor [29]) and chamomile. Paracellular transport would not be affected by any of the tested compounds or extracts, and since paracellular transport of glucose is negligible [38], this would allow glucose transport to be effectively inhibited. Indeed, in some cases inhibition of glucose transport at high concentrations of chamomile or green tea reached ~90%. When deoxy-D-glucose was used as the test substrate, substantial inhibition was observed, since this substrate is not metabolized further after entry into the cell, and is transported by SGLT1 and GLUT2, but not GLUT5 [39-41]. In our models we confirmed that the drug acarbose does not inhibit any of the transport components tested, which supports the hypothesis that it could act synergistically with the chamomile or green tea on carbohydrate digestive processes in vivo (Figure 9), and the work presented here opens the door to further in vivo studies.

Very few compounds have been shown to directly inhibit GLUT5. Although eucalyptus leaf extract inhibited fructose absorption in rats and suppressed sucrose-induced adiposity [42], in our hands eucalyptus extract showed no inhibition of human GLUT5 in oocytes (data not shown). GLUT5 is only weakly inhibited by chamomile and, given its involvement in fructose transport, only partial and not total inhibition of fructose absorption in the intestine can be anticipated. This implies that the effect reported here would not lead to fructose malabsorption, as fructose is not fully inhibited even with very strong chamomile tea or green tea. Instead, any attenuation in vivo would allow time for the liver to process fructose, prevent the inundation, and suppress dramatic changes in ATP levels that can activate lipogenesis and overwhelm mitochondrial circuits. Thus chamomile and green teas, which consist of a

multitude of bioactive agents, could attenuate fructose absorption, which the drug acarbose cannot achieve. These results can help in the development of combined interventions enabling diabetics to manage their condition, as well as providing preventative dietary strategies to curtail hyperglycaemic stress.

Figure legends:

Figure 1. Sugar transport across differentiated Caco-2 monolayers. Panel A shows the time course of transport of 5 mM D-[^{14}C(U)]-fructose from the apical to basolateral side of differentiated Caco-2 monolayers. Panel B shows the amount of intracellular D-[^{14}C(U)]-fructose after treatment of cells with 5 mM D-[^{14}C(U)]-fructose. Panel C shows the time course of transport of 1 mM D-[^{14}C(U)]-glucose from the apical to basolateral side of differentiated Caco-2 monolayers. Panel D shows the amount of intracellular D-[^{14}C(U)]-glucose after treatment of cells with 1 mM D-[^{14}C(U)]-glucose. Panel E show the time course of transport of 5 mM [^{14}C(U)]-sucrose from the apical to basolateral side of differentiated Caco-2 monolayers. Panel F shows the transport of different applied concentrations of [^{14}C(U)]-sucrose from apical to basolateral (■), and from basolateral to apical (○) compartments of differentiated Caco-2 monolayers. Different letters denote statistical differences between data points (p≤0.01). Stars denote significant differences between the compared data points (***p≤0.001). Where not visible, error bars are smaller than the size of the data point; values are mean ± SD (n=6 independent determinations). Transport of glucose is comparable to previously published data [43].

Figure 2. Inhibition of sugar transport across differentiated Caco-2 monolayers. Panel A shows the effect of chamomile (1 mg/ml) on D-[^{14}C(U)]-fructose transport across differentiated Caco-2 cell monolayers at different applied fructose concentrations. Stars indicate significant differences between chamomile (■) and control (□) (***p ≤0.001), and letters indicate significant differences between the applied concentrations of fructose (p ≤0.01). The effect of chamomile on [^{14}C]-labelled-sugar transport across differentiated Caco-2 cell monolayers from apical to basolateral compartments is shown in panel B (1 mM D-[^{14}C(U)]-glucose), in panel C (5 mM D-[^{14}C(U)]-fructose) and in panel D (5 mM [^{14}C(U)]-

sucrose). From this data, the IC_{50} values were calculated and shown in Table 1. For panels B-D, letters denote differences between data points at the level of significance indicated in the panel. Where not visible, error bars are smaller than the size of the data point, which is mean $\pm$ SD (n=4-6 independent determinations).

Figure 3. Analysis of chamomile by LC-MS/MS. Top panel shows the UV traces of chamomile (0.1 mg/ml) at 280 and 340 nm and subsequent overlaid SRM traces of major individual components and transitions used for quantification according to Table 3.

Figure 4. Deoxy-D-glucose transport across, and uptake into, differentiated Caco-2 monolayers. Effect of extracts (1 mg/ml) on 2-[^{14}C(U)]-deoxy-D-glucose (1 mM) transport (panel A) and cellular uptake (panel B). Values are shown as mean $\pm$ SD (n=6). Letters denote significant differences between groups (p≤0.01). GT, green tea; Cham, chamomile.

Figure 5. **Inhibition of glucose transport across differentiated Caco-2/TC7 monolayers.** Panel A shows dose-dependent inhibition of D-[^{14}C(U)]-glucose transport by phloridzin (■) and phloretin (●) in TBS containing Na^+; differences between phloridzin and phloretin indicated by * p≤0.05; ** p≤0.01. Panel B shows chemical structures of phloridzin (top structure) and phloretin (lower structure). Panel C shows D-[^{14}C(U)]-glucose transport under Na^+ (black bars) and Na^+-free conditions (light grey bars) in the presence of 200 µM phloridzin (dark grey bars), * p≤0.05. Panel D shows dose-dependent inhibition of D-[^{14}C(U)]-glucose transport by chamomile under Na^+ and Na^+-free conditions by phloridzin (■) and phloretin (●); differences between Na^+ against Na^+-free indicated by * p≤0.05; ** p≤0.01. All data shown are mean $\pm$ SD (n=6). When not visible, the error bars are smaller than the data point.

Figure 6. **GLUT5 expression in differentiated Caco-2 and Caco-2/TC7 cell monolayers.**

Standard curves for multiplexed GLUT5 and Claudin-1 using different concentrations of total cell lysate from Caco-2 (panel A) and Caco-2/TC7 cells (panel B) were obtained using quantitative capillary Western blotting (WES). Electropherogram view (panel C) and gel-like reconstructed image (D) for representative samples are shown using equivalent concentrations of cell lysate (0.1 mg/ml). Panel E shows GLUT5 protein expression in Caco-2 and Caco-2/TC7 cells for 2 seeding experiments repeated with three biological replicates and analysed in triplicate. * $p \leq 0.05$, ** $p \leq 0.01$. Given the large difference in protein expression of Claudin-1 between the two cell lines (13-fold), we have presented the peak areas of GLUT5 in CaCo-2 and CaCo-2/ TC7 cells without normalization to Claudin-1, but normalized instead to total protein. Panel F shows GLUT5 mRNA in differentiated Caco-2 and Caco-2/TC7 cell monolayers measured using digital droplet PCR.

Figure 7. Effect of compounds on sugar uptake by Xenopus oocytes expressing GLUT2 or GLUT5. Panel A shows the effect of L-sorbose-Bn-OZO on uptake of 5 mM D-[^{14}C(U)]-fructose by Xenopus oocytes expressing GLUT5. Panel B shows that acarbose has no significant effect on uptake of D-[^{14}C(U)]-glucose or D-[^{14}C(U)]-fructose by Xenopus oocytes expressing GLUT2 with 0.1 mM glucose (black bars), or on GLUT5 with 0.1 mM (dark grey bars) or 5 mM fructose (light grey bars). Panel C shows the effect of green tea (GT) on uptake of D-[^{14}C(U)]-fructose or D-[^{14}C(U)]-glucose by Xenopus oocytes expressing GLUT5 with 0.1 mM fructose (black bars) or GLUT2 with 0.1 mM glucose (grey bars). Panel D shows the effect of chamomile on 0.1 mM D-[^{14}C(U)]-fructose uptake into Xenopus oocytes expressing human GLUT5 one day post cDNA microinjection compared to water injected controls. Each data point represents >6 independent replicates of 3 oocytes per data

point showing the mean ± SD. Panel E shows the effect of chamomile on 5 mM D-[^{14}C(U)]-fructose uptake into Xenopus oocytes expressing human GLUT5 one day post cDNA microinjection compared to water injected controls. Each data point represents 3 independent replicates of 3 oocytes per data point showing mean ± SD. Panel F shows the effect of chamomile on 0.1 mM [^{14}C]-labelled-glucose uptake into Xenopus oocytes expressing human GLUT2 two days post cDNA microinjection compared to water injected controls. Each data point represents >6 independent replicates of 3 oocytes per data point showing the mean ± SD.

Figure 8: Effect of acute and chronic chamomile treatments on sugar transport across and into differentiated Caco-2 monolayers. Cells were treated with chamomile (1 mg/ml) for 16 h and at the end of this period, the medium was replaced with D-[^{14}C(U)]-glucose (1 mM), D-[^{14}C(U)]-fructose (5 mM) or [^{14}C(U)]-sucrose (5 mM) sugar as indicated, with and without chamomile for the duration of the transport experiment using. Apical to basolateral transport (panel A) and intracellular content (panel B) was measured by scintillation counting. Cells were similarly treated with chamomile for 96 h, and apical to basolateral transport measured in the absence of chamomile (panel C). * p≤0.05.

Figure 9. **Summary of the proposed mechanism for chamomile (Cham) and acarbose (Acar)**. Sites of observed inhibition are indicated by white rectangles; chamomile inhibition of maltase activity is weak and not included.

Figures
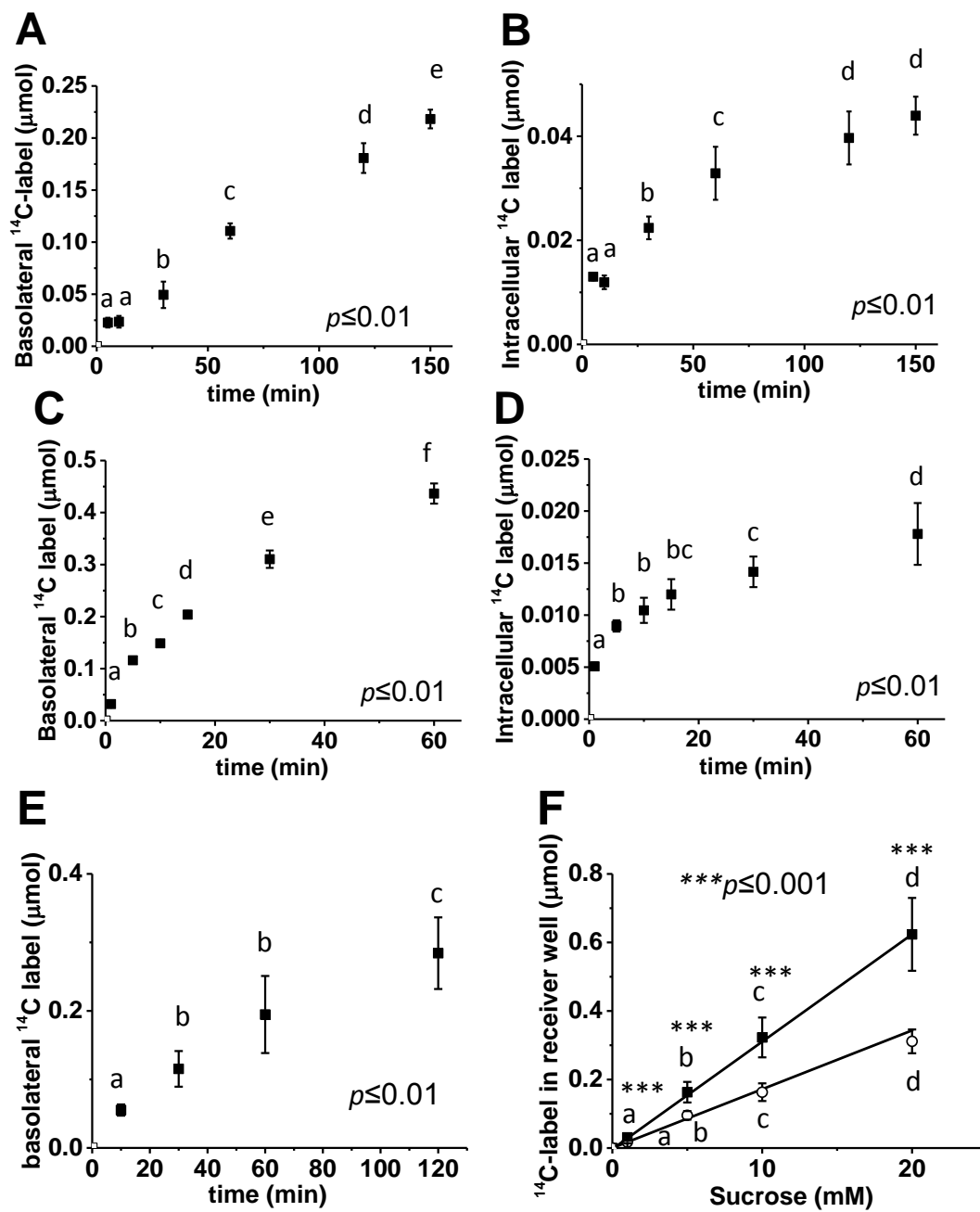
Figure 1
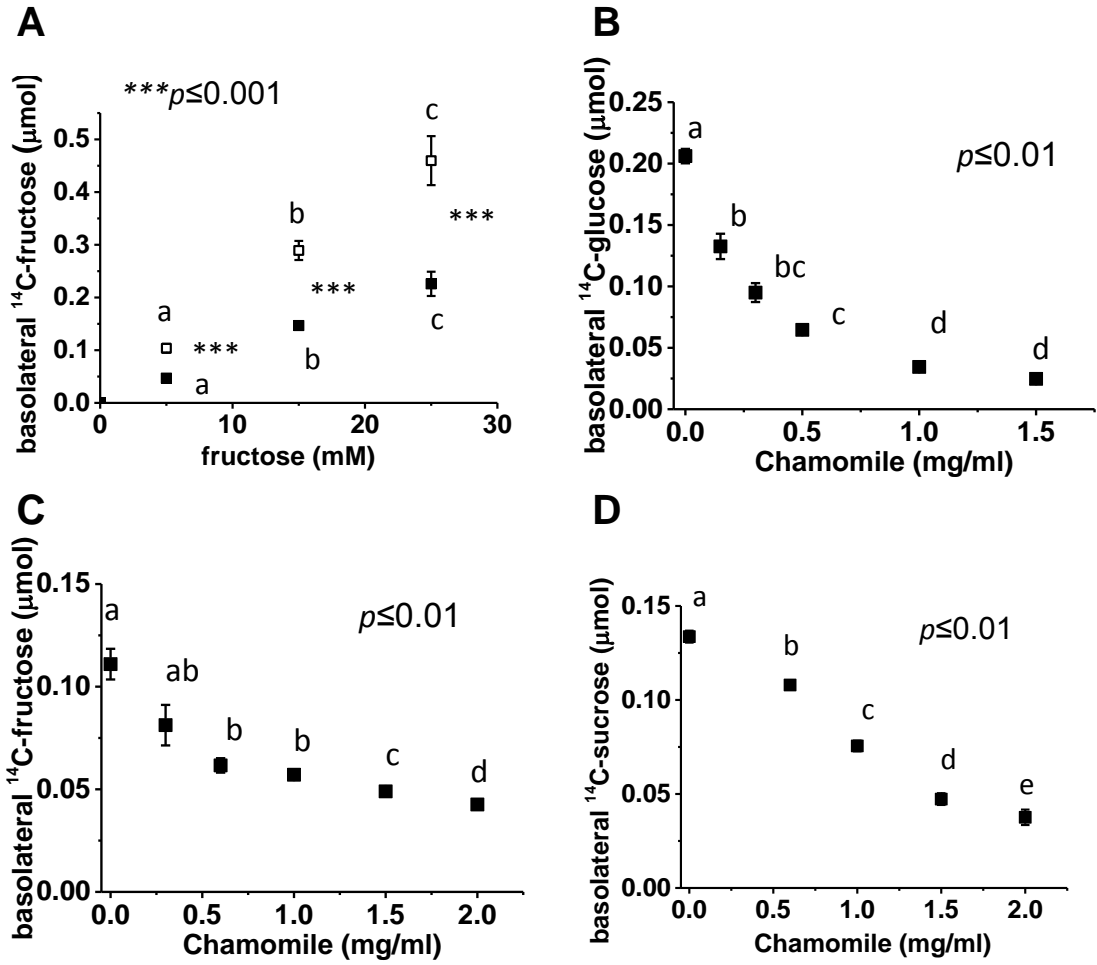
Figure 2
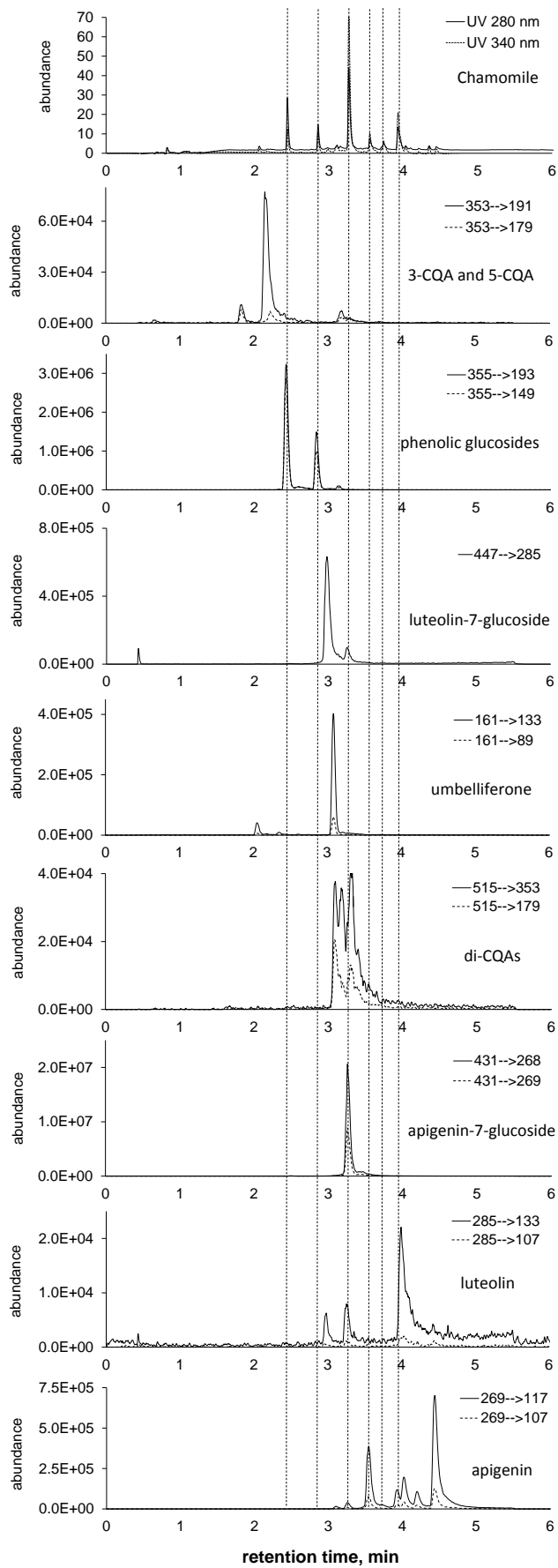
Figure 3
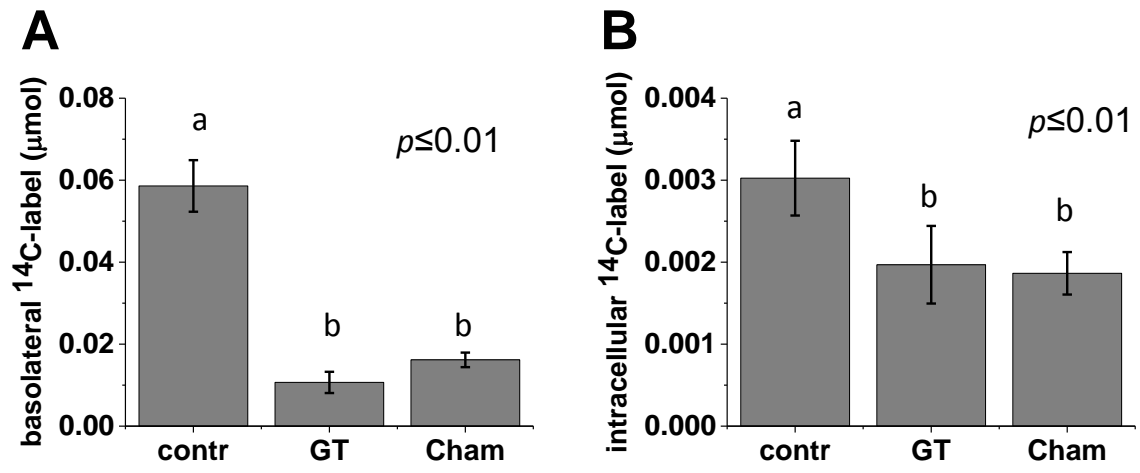
Figure 4
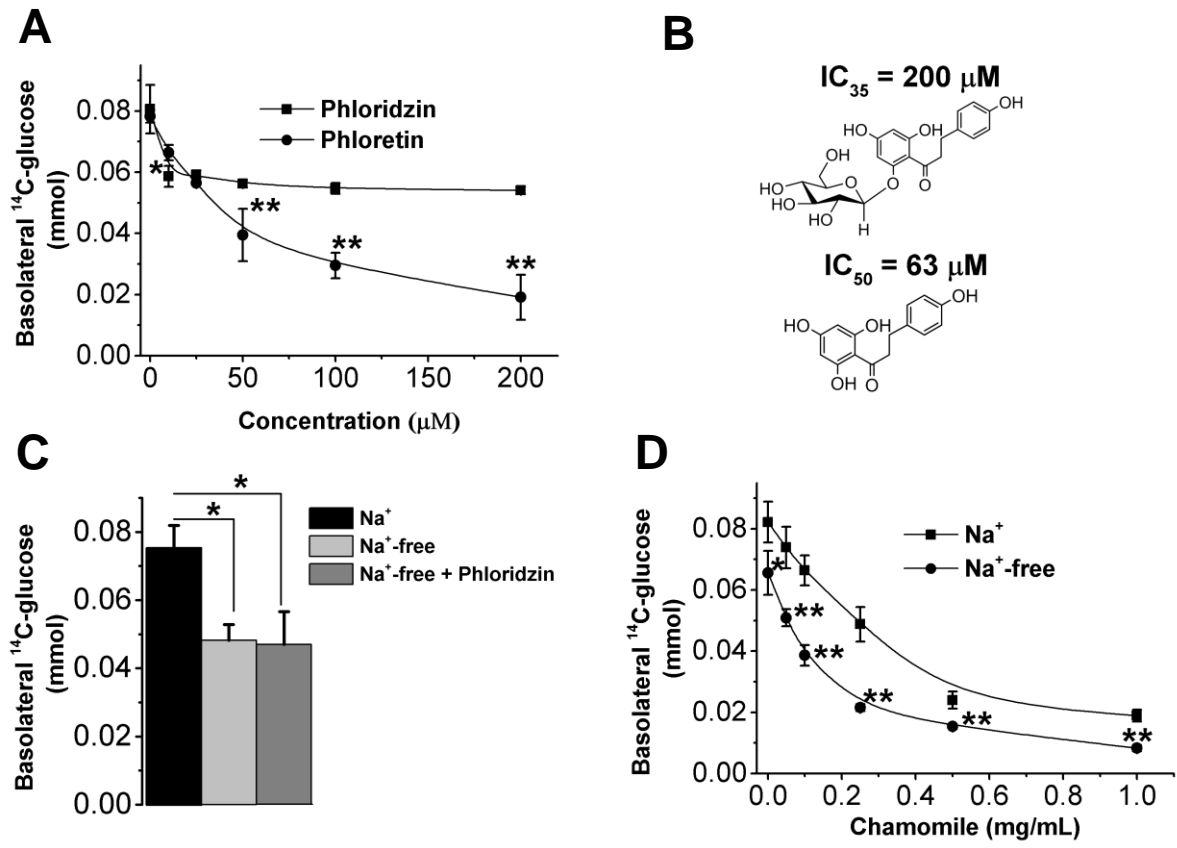
**Figure 5**
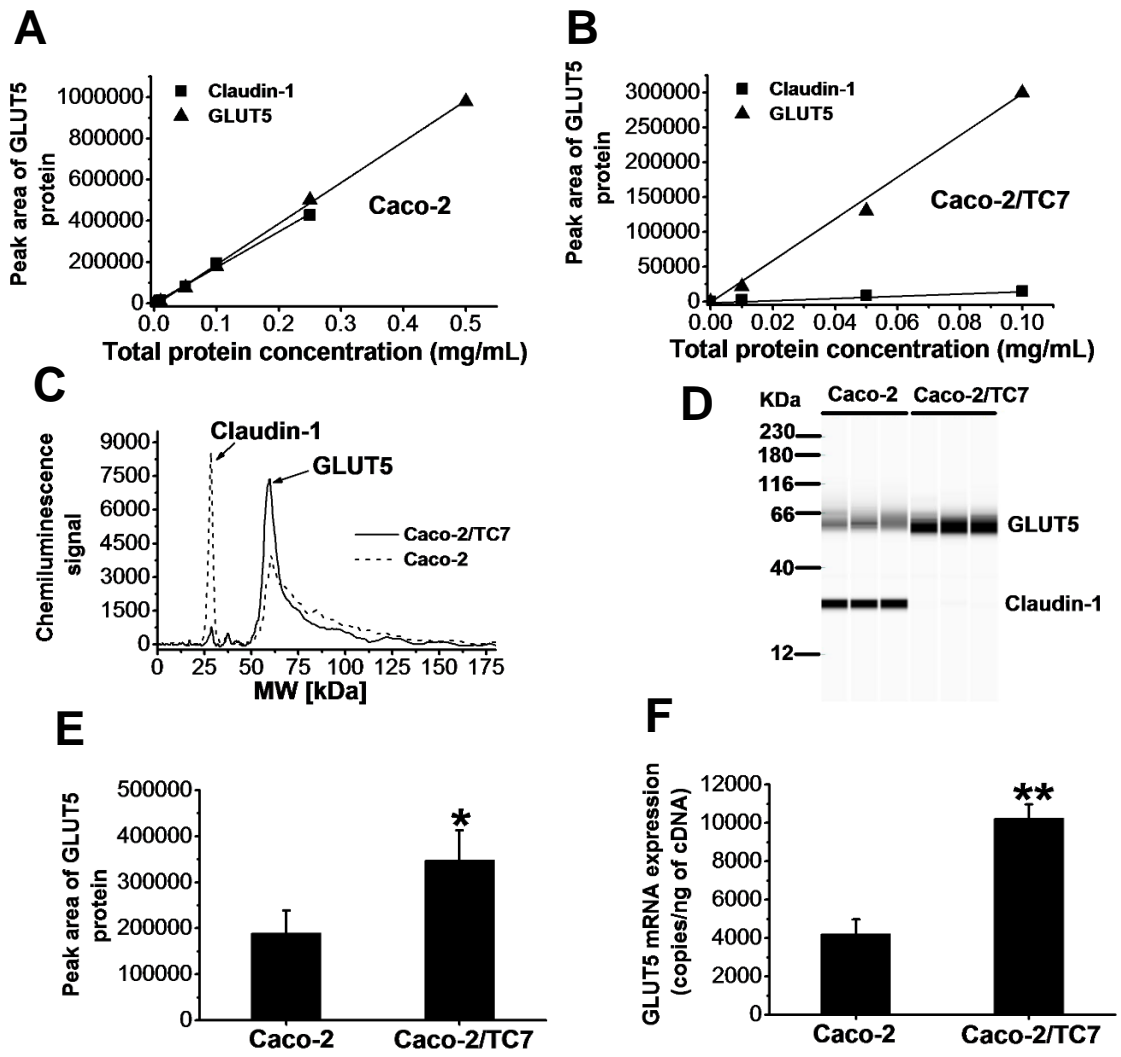
Figure 6
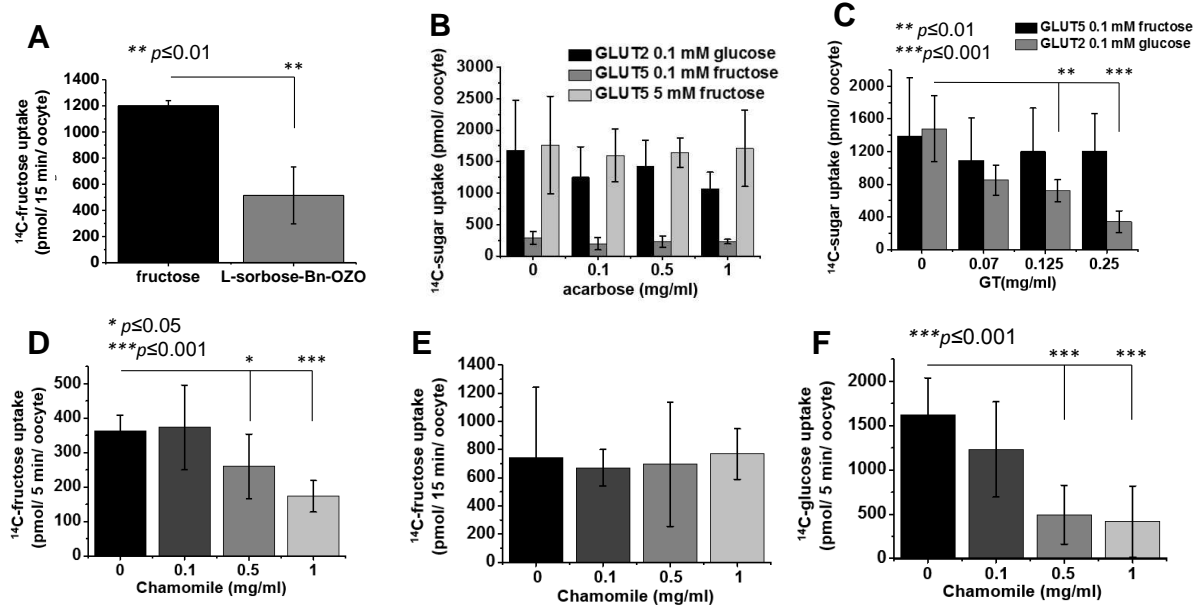
Figure 7
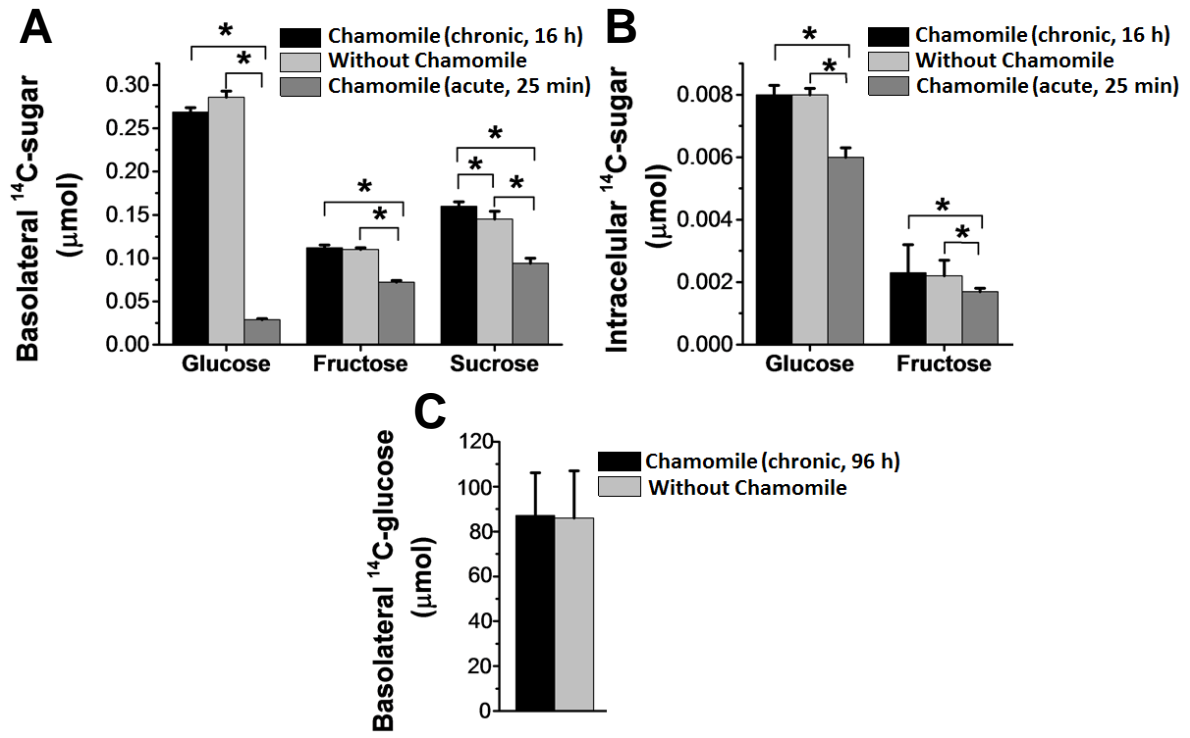
Figure 8
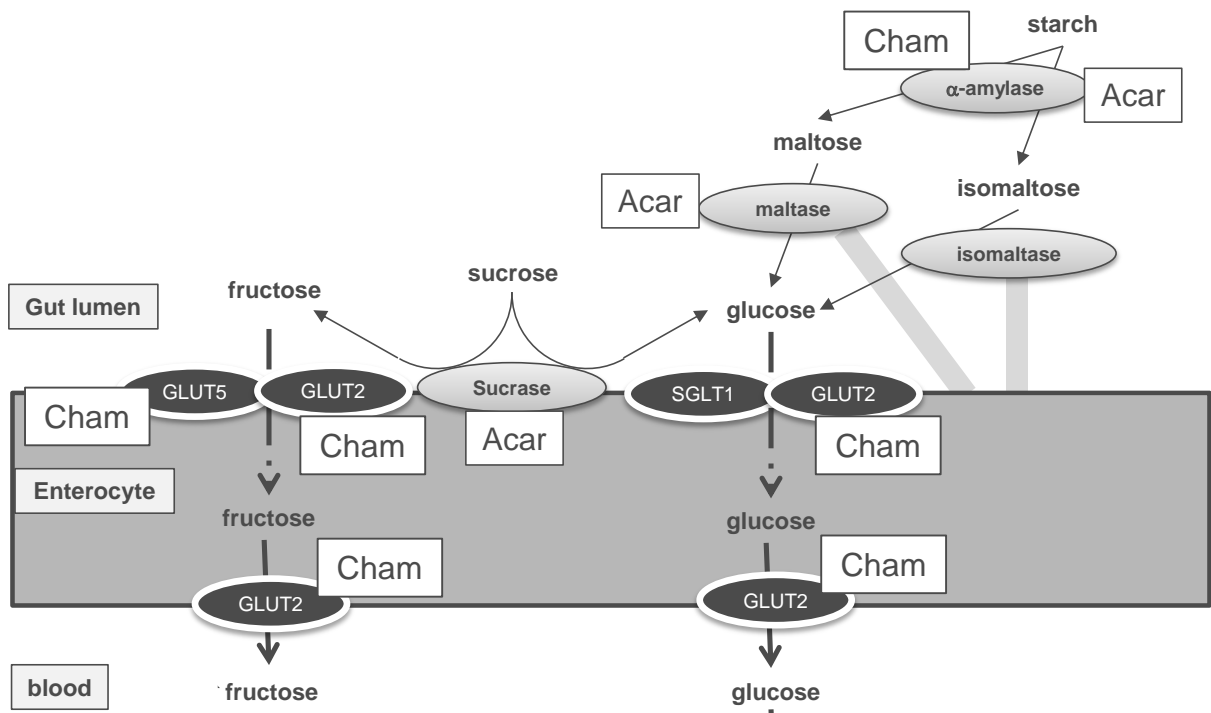
Figure 9

Tables:

Table 1. **Effect of acarbose and herbal extracts on transport and uptake of glucose (1 mM), fructose (5 mM) and sucrose (5 mM) across differentiated Caco-2 cell monolayers**.

Tested compound or extract	D-[^{14}C(U)]- glucose transport	D-[^{14}C(U)]- glucose uptake	D-[^{14}C(U)]- fructose transport	D-[^{14}C(U)]- fructose uptake	[^{14}C(U)]- sucrose transport	[^{14}C(U)]- sucrose transport[1]
Chamomile	0.32 ± 0.05	$0.5\,2 \pm 0.12$	1.0 ± 0.12	2.0 ± 0.17	1.12 ± 0.17	0.56 ± 0.035
Green tea	0.26 ± 0.04	0.55 ± 0.17	0.8 ± 0.09	0.7 ± 0.08	0.98 ± 0.12	0.32 ± 0.05
Acarbose	NI	-	NI	-	-	7.0 ± 3

[1]In Caco-2/TC7 cells, which express higher levels of brush border sucrase.

NI = no inhibition observed up to 0.5 mM. Data shown are IC_{50} values in mg extract/ml medium for plant extracts and in µM for acarbose.

Table 2. Analysis of chamomile extract used for most abundant phenolic components

	RT (min)	$[M-H]^-$ (m/z)	MS^2 (m/z)	concentration (% dry weight)[1]
3-CQA	1.84	353	191	0.01
5-CQA	2.17	353	179	0.07
phenolic glucoside(s)[2]	2.44	355	193	_
phenolic glucoside(s)[2]	2.85	355	149	_
luteolin-7-O-glucoside	2.99	447	285	0.13
umbelliferone	3.09	161	133, 89	0.09
di-CQAs	3.10; 3.19; 3.31	515	353, 179	0.13
apigenin-7-O-glucoside	3.27	431	268, 269	12.3
luteolin	4.00	285	133, 107	0.01
apigenin	4.44	269	117, 107	0.28

[1]excluding maltodextrin content.

[2]No available standards for phenolic glucosides, which have not been conclusively identified in the literature. CQA, caffeoylquinic acid.

1   **Table 3: Summary of inhibition of α-amylase, maltase, isomaltase, sucrase, GLUT2 and GLUT5 activities.**

	Substrate for human salivary α-amylase	Inhibition (IC$_{50}$)	Rat intestinal enzyme[1]	Inhibition (IC$_{50}$)	Human enzyme or transporter[2]	Inhibition
Chamomile	amylopectin	0.95 ± 0.038 mg/ml	maltase	28 ± 1.8% at 1 mg/ml	GLUT5 (fructose)	NI at [F] = 5 mM IC$_{50}$ = 0.73 ± 0.18 mg/ml at [F] = 0.1 mM
	amylose	0.29 ± 0.05 mg/ml	isomaltase	NI[3]	sucrase	NI
			sucrase	NI[3]	GLUT2 (glucose)	IC$_{50}$ = 0.54 ± 0.24 mg/ml at [G] = 5 mM
Acarbose	amylopectin	9.23 ± 0.75 μM	maltase	0.42 ± 0.01 μM	GLUT5 (fructose)	NI at [F]= 0.1 and 5 mM
	amylose	3.45 ± 0.18 μM	isomaltase	440 ± 79 μM	Sucrase	57±11 % at 10 μM
			sucrase	6.7 ± 1.5 μM	GLUT2 (glucose)	NI at [G] = 5 mM
Green tea	amylopectin	0.022 ± 0.001 mg/ml	maltase	0.44 ± 0.09 mg/ml	GLUT5 (fructose)	NI at [F] = 0.1 and 5 mM
	amylose	0.0093 ± 0.003 mg/ml	isomaltase	0.69 ± 0.15 mg/ml	sucrase	32 ± 7% at 0.5-5 mg/ml (plateau)
			sucrase	0.95 ± 0.12 mg/ml	GLUT2 (glucose)	IC$_{50}$ = 0.13 ± 0.02 mg/ml at [G] = 5 mM

2

3   NI=no inhibition; an IC_{50} value is the concentration required for 50% inhibition; [F] and [G] are fructose and glucose substrate concentrations

4   respectively; substrate for sucrase is sucrose.

5   [1]For the protein extract from rat intestine, apparent K_m values were 3.4, 5.7 and 18 mM for maltose, isomaltose and sucrose respectively. All

6   inhibition assays were performed in the linear part of the time and dose curves.

7   [2]Human GLUT2 and GLUT5 expressed in Xenopus oocytes; sucrase as a cell-free extract from Caco-2 TC7 cells.

8   [3]Maximum concentration of extract tested was 1 mg/ml

9   For sucrase inhibition: acarbose, 4 experiments in triplicate (n=12); green tea, 2 experiments in triplicate (n = 6). For GLUT2 and GLUT5

10   expressed in Xenopus oocytes, 6 replicates of 3 oocytes for each data point. For α-amylase inhibition, 3 independent experiments with 3

11   technical replicates (n = 9).

12

13

References

[1] Barone, S., Fussell, S. L., Singh, A. K., Lucas, F., Xu, J., Kim, C., Wu, X., Yu, Y., Amlal, H., Seidler, U., Zuo, J., Soleimani, M., Slc2a5 (Glut5) is essential for the absorption of fructose in the intestine and generation of fructose-induced hypertension. J. Biol. Chem. 2009, 284, 5056-5066.

[2] Stanhope, K. L., Schwarz, J. M., Havel, P. J., Adverse metabolic effects of dietary fructose: results from the recent epidemiological, clinical, and mechanistic studies. Curr. Opin. Lipidol. 2013, 24, 198-206.

[3] Lanaspa, M. A., Sanchez-Lozada, L. G., Cicerchi, C., Li, N. Roncal-Jimenez, C.A., Ishimoto, T., Le, M., Garcia, G.E., Thomas, J.B., Rivard, C.J., Andres-Hernando, A., Hunter, B., Schreiner, G., Rodriguez-Iturbe, B., Sautin, Y.Y., Johnson, R.J., Uric acid stimulates fructokinase and accelerates fructose metabolism in the development of fatty liver. PLoS. ONE 2012, 7, e47948.

[4] Lanaspa, M. A., Cicerchi, C., Garcia, G., Li, N. Roncal-Jimenez, C.A., Rivard, C.J., Hunter, B., Andres-Hernando, A., Ishimoto, T., Sanchez-Lozada, L.G., Thomas, J., Hodges, R.S., Mant, C.T., Johnson, R.J., Counteracting roles of AMP deaminase and AMP kinase in the development of fatty liver. PLoS. ONE 2012, 7, e48801.

[5] Sun, S. Z., Flickinger, B. D., Williamson-Hughes, P. S., Empie, M. W., Lack of association between dietary fructose and hyperuricemia risk in adults. Nutr. Metab. 2010, 7, 16. doi: 10.1186/1743-7075-7-16.

[6] Bhupathiraju, S. N., Tobias, D. K., Malik, V. S., Pan, A. Hruby, A., Manson, J.E., Willett, W.C., Hu, F.B., Girniene, J., Tatibouet, A., Sackus, A., Yang, J., Holman, G.D., Rollin, P., Glycemic index, glycemic load, and risk of type 2 diabetes: results from 3 large US cohorts and an updated meta-analysis. Am. J. Clin. Nutr. 2014, 100, 218-232.

[7] Livesey, G., Taylor, R., Hulshof, T., Howlett, J., Glycemic response and health--a systematic review and meta-analysis: relations between dietary glycemic properties and health outcomes. Am. J. Clin. Nutr. 2008, 87, 258S-268S.

[8] Su, Y., Liu, X. M., Sun, Y. M., Wang, Y. Y. Luan, Y., Wu, Y., Endothelial dysfunction in impaired fasting glycemia, impaired glucose tolerance, and type 2 diabetes mellitus. Am. J. Cardiol. 2008, 102, 497-498.

[9] Quagliaro, L., Piconi, L., Assaloni, R., Da, R. R., Szabo, C., Ceriello, A., Primary role of superoxide anion generation in the cascade of events leading to endothelial dysfunction and damage in high glucose treated HUVEC. Nutr. Metab Cardiovasc. Dis. 2007, 17, 257-267.

[10] Sim, L., Willemsma, C., Mohan, S., Naim, H. Y., Pinto, B.M., Rose, D.R., Structural basis for substrate selectivity in human maltase-glucoamylase and sucrase-isomaltase N-terminal domains. J. Biol. Chem. 2010, 285, 17763-17770.

[11] Zeymer, U., Cardiovascular benefits of acarbose in impaired glucose tolerance and type 2 diabetes. Int. J. Cardiol. 2006, 107, 11-20.

[12] Vargas-Murga, L., Garcia-Alvarez, A., Roman-Vinas, B., Ngo, J., Ribas-Barba, L., van den Berg, S.J., Williamson, G., Serra-Majem, L., Plant food supplement (PFS) market structure in EC Member States, methods and techniques for the assessment of individual PFS intake. Food Funct. 2011, 2, 731-739.

[13] Suksomboon, N., Poolsup, N., Boonkaew, S., Suthisisang, C. C., Meta-analysis of the effect of herbal supplement on glycemic control in type 2 diabetes. J. Ethnopharmacol. 2011, 137, 1328-1333.

[14] Sun, S. Z., Empie, M. W., Fructose metabolism in humans - what isotopic tracer studies tell us. Nutr. Metab. 2012, 9, 89. doi: 10.1186/1743-7075-9-89.

[15] Williamson, G., Possible effects of dietary polyphenols on sugar absorption and digestion. Mol. Nutr. Food Res. 2013, 57, 48-57.

[16] Kato, A., Minoshima, Y., Yamamoto, J., Adachi, I., Watson, A. A., Nash, R. J., Protective effects of dietary chamomile tea on diabetic complications. J. Agric. Food Chem. 2008, 56, 8206-8211.

[17] Weidner, C., Wowro, S. J., Rousseau, M., Freiwald, A., Kodelja, V., Abdel-Aziz, H., Kelber, O., Sauer, S., Antidiabetic effects of chamomile flowers extract in obese mice through transcriptional stimulation of nutrient sensors of the peroxisome proliferator-activated receptor (PPAR) family. PLoS. ONE 2013, 8, e80335.

[18] Zemestani, M., Rafraf, M., Asghari-Jafarabadi, M., Chamomile tea improves glycemic indices and antioxidants status in patients with type 2 diabetes mellitus. Nutrition 2016, 32, 66-72.

[19] Venables, M. C., Hulston, C. J., Cox, H. R., Jeukendrup, A. E., Green tea extract ingestion, fat oxidation, and glucose tolerance in healthy humans. Am. J. Clin. Nutr. 2008, 87, 778-784.

[20] Snoussi, C., Ducroc, R., Hamdaoui, M. H., Dhaouadi, K. Abaidi, H., Cluzeaud, F., Nazaret, C., Le, G. M., Bado, A., Green tea decoction improves glucose tolerance and reduces weight gain of rats fed normal and high-fat diet. J. Nutr. Biochem. 2014, 25, 557-564.

[21] Forester, S. C., Gu, Y., Lambert, J. D., Inhibition of starch digestion by the green tea polyphenol, (-)-epigallocatechin-3-gallate. Mol. Nutr. Food Res. 2012, 56, 1647-1654.

[22] Mahraoui, L., Rodolosse, A., Barbat, A., Dussaulx, E., Zweibaum, A., Rousset, M., Brot-Laroche, E., Presence and differential expression of SGLT1, GLUT1, GLUT2, GLUT3 and GLUT5 hexose-transporter mRNAs in Caco-2 cell clones in relation to cell growth and glucose consumption. Biochem. J. 1994, 298, 629-633.

[23] Mahraoui, L., Rousset, M., Dussaulx, E., Darmoul, D. Zweibaum, A. Brot-Laroche, E., Expression and localization of GLUT-5 in Caco-2 cells, human small intestine, and colon. Am. J. Physiol. 1992, 263, G312-G318.

[24] Ellwood, K. C., Chatzidakis, C., Failla, M. L., Fructose utilization by the human intestinal epithelial cell line, Caco-2. Proc. Soc. Exp. Biol. Med. 1993, 202, 440-446.

[25] Zheng, Y., Scow, J. S., Duenes, J. A., Sarr, M. G., Mechanisms of glucose uptake in intestinal cell lines: role of GLUT2. Surgery 2012, 151, 13-25.

[26] Grefner, N. M., Gromova, L. V., Gruzdkov, A. A., Komissarchik, I., [Caco 2 cell culture as intestinal epithelium model for hexose transport studying]. Tsitologiia 2012, 54, 318-323.

[27] Nyambe-Silavwe, H., Villa-Rodriguez, J. A., Ifie, I., Holmes, M., Aydin, E., Jensen, J.M., Williamson, G., Inhibition of human alpha-amylase by dietary polyphenols. J. Funct. Foods 2015, 19, 723-732.

[28] Gao, H., Huang, Y. N., Xu, P. Y., Kawabata, J., Inhibitory effect on alpha-glucosidase by the fruits of Terminalia chebula Retz. Food Chem. 2007, 105, 628-634.

[29] Kwon, O., Eck, P., Chen, S., Corpe, C. P., Lee, J. H., Kruhlak, M., Levine, M., Inhibition of the intestinal glucose transporter GLUT2 by flavonoids. FASEB J. 2007, 21, 366-377.

[30] Walle, T., Walle, U. K., The beta-D-glucoside and sodium-dependent glucose transporter 1 (SGLT1)-inhibitor phloridzin is transported by both SGLT1 and mulitdrug resistance-associated protiens 1/2. Drug Metab. Dispo.s 2003, 31, 1288-1291.

[31] Helliwell, P. A., Richardson, M., Affleck, J., Kellett, G. L., Stimulation of fructose transport across the intestinal brush-border membrane by PMA is mediated by GLUT2 and dynamically regulated by protein kinase C. Biochem. J. 2000, 350, 149-154.

[32] Girniene, J., Tatibouet, A., Sackus, A., Yang, J. Holman, G. D., Rollin P., Inhibition of the D-fructose transporter protein GLUT5 by fused-ring glyco-1,3-oxazolidin-2-thiones and -oxazolidin-2-ones. Carbohydr. Res. 2003, 338, 711-719.

[33] Johnson, R. J., Perez-Pozo, S. E., Sautin, Y. Y., Manitius, J. Sanchez-Lozada, L. G., Feig, D. I., Shafiu, M., Segal, M., Glassock, R.J., Shimada, M., Roncal, C., Nakagawa, T.,

Hypothesis: could excessive fructose intake and uric acid cause type 2 diabetes? Endocr. Rev. 2009, 30, 96-116.

[34] Jenkins, D. J., Taylor, R. H., Goff, D. V., Fielden, H. Misiewicz, J. J., Sarson, D. L., Bloom, S. R., Alberti, K. G., Scope and specificity of acarbose in slowing carbohydrate absorption in man. Diabetes 1981, 30, 951-954.

[35] Paiva, L., Binsack, R., Machado, U. F., Chronic acarbose-feeding increases GLUT1 protein without changing intestinal glucose absorption function. Eur. J. Pharmacol. 2002, 434, 197-204.

[36] Madariaga, H., Lee, P. C., Heitlinger, L. A., Lebenthal, E., Effects of graded alpha-glucosidase inhibition on sugar absorption in vivo. Dig. Dis. Sci. 1988, 33, 1020-1024.

[37] Turk, E., Zabel, B., Mundlos, S., Dyer, J., Wright, E. M., Glucose/galactose malabsorption caused by a defect in the Na+/glucose cotransporter. Nature 1991, 350, 354-356.

[38] Kellett, G. L., Helliwell, P. A., The diffusive component of intestinal glucose absorption is mediated by the glucose-induced recruitment of GLUT2 to the brush-border membrane. Biochem. J. 2000, 350, 155-162.

[39] Arbuckle, M. I., Kane, S., Porter, L. M., Seatter, M. J., Gould, G. W., Structure-function analysis of liver-type (GLUT2) and brain-type (GLUT3) glucose transporters: expression of chimeric transporters in Xenopus oocytes suggests an important role for putative transmembrane helix 7 in determining substrate selectivity. Biochemistry 1996, 35, 16519-16527.

[40] Kanwal, A., Singh, S. P., Grover, P., Banerjee, S. K., Development of a cell-based nonradioactive glucose uptake assay system for SGLT1 and SGLT2. Anal. Biochem. 2012, 429, 70-75.

[41] Kane, S., Seatter, M. J., Gould, G. W., Functional studies of human GLUT5: effect of pH on substrate selection and an analysis of substrate interactions. Biochem. Biophys. Res. Commun. 1997, 238, 503-505.

[42] Sugimoto, K., Suzuki, J., Nakagawa, K., Hayashi, S., Enomoto, T., Fujita, T., Yamaji, R., Inui, H., Nakano, Y., Eucalyptus leaf extract inhibits intestinal fructose absorption, and suppresses adiposity due to dietary sucrose in rats. Br. J. Nutr. 2005, 93, 957-963.

[43] Manzano, S., Williamson, G., Polyphenols and phenolic acids from strawberry and apple decrease glucose uptake and transport by human intestinal Caco-2 cells. Mol. Nutr. Food Res. 2010, 54, 1773-1780.